ELECTROMAGNETICALLY ACTUATED BALL VALVE MICROPUMPS

Christophe Yamahata, Frédéric Lacharme, Jan Matter, Silvan Schnydrig, Yves Burri, and Martin A. M. Gijs

Institute of Microelectronics and Microsystems,
Ecole Polytechnique Fédérale de Lausanne (EPFL), Switzerland
e-mail: christophe.yamahata@a3.epfl.ch

ABSTRACT

We present two types of oscillating diaphragm micropumps configured with passive ball valves and using electromagnetic actuation. One type is made out of poly(methyl methacrylate) (PMMA), while the other one is made out of borosilicate glass. Both were produced using the powder blasting microfabrication method. The pumping resonant frequency was measured to be within the range of 20 – 30 Hz for both prototypes. At the resonance, a maximum back-pressure of 280 mbar and a maximum water flow rate of about 5 mL/min were obtained. The experimental results can be well described by a simple hydrodynamic model of the system.

Keywords: Ball valve, Micropump, Magnetic actuation, PMMA, Glass

1. INTRODUCTION

Reciprocating micropumps consist of an oscillating membrane (or piston) and two valves placed at the inlet and outlet of the pumping chamber for rectification of the flow. The valves are the most critical element since their leakage causes the pumps to be less performing in terms of back-pressure and flow rate. Although ball valves are excellent candidates for the generation of an unidirectional flow, they have been rarely used in microfluidic systems. Among the hundreds of micropumps presented in literature [1,2], only a few ones have been reported employing ball valves. This might be due to their non-trivial combination with classical two-dimensional microfabrication techniques. Ball valves have been used in either micropumps or as individual fluidic components.

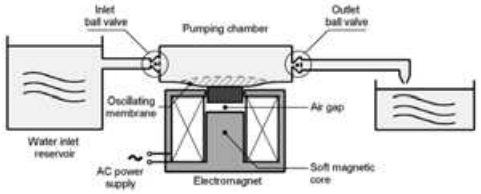

Fig. 1. Schematic diagram of the ball valve micropump with

Ball valve micropumps. A first type of piezoelectrically actuated micropump with passive ball valves was developed by Carrozza *et al.* [3]. It was made by stereolithography and comprised steel balls of diameter (Ø) 1.2 mm. Later, Feustel *et al.* presented a silicon/glass micropump with passive ball valves [4]. It was fabricated by KOH and plasma etching of silicon combined with HF microstructuring of borosilicate glass. In their design, they used Ø 200 µm steel balls and they actuated the membrane with a piezoelectric bimorph. Recently, a ball valve micropump in PMMA with a pneumatically actuated poly(dimethylsiloxane) (PDMS) membrane was proposed by Sin *et al.* [5]. Here, they integrated Ø 400 µm synthetic ruby balls. In a forthcoming article, Pan *et al.* present the PDMS-based fabrication method of a magnetically actuated micropump with passive ball valves [6]. In their approach, Ø 0.8 mm steel balls are entrapped into teflon microtubes. Finally, a multilayered ceramic micropump including either passive or active ball valves was reported in patent literature [7].

Active ball valves. Usually, discrete microvalves to be used in fluid flow control are active elements [8]. Krusemark *et al.* demonstrated the potential use of an electromagnetically actuated steel ball valve [9], which was also used in an alternate design of their micropump [4]. Fu *et al.* [10] presented electromagnetically controlled miniature (Ø 3 mm) steel ball valves produced by multilayer adhesive bonding of metal and polymer films.

In this paper, we present the fabrication of two types of electromagnetically actuated micropumps with passive ball valves. In both cases, Ø 0.7 mm stainless steel balls were used. For the fabrication of our prototypes in (i) PMMA and (ii) glass, we used a simple powder blasting process. A back-pressure as high as 280 mbar and water flow rates up to 5 mL/min were obtained thanks to the large magnetic actuation force and the use of high-efficiency ball valves. The frequency-dependent flow characteristics of the fabricated micropumps are explained using a hydrodynamic damped oscillator model.

2. WORKING PRINCIPLE

The reciprocating micropumps presented hereafter are of the diaphragm type and comprise two passive

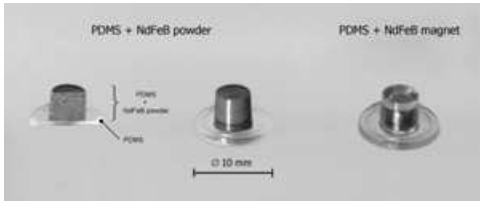

Fig. 2. PDMS membrane with integrated magnet. The left photograph shows the PDMS membrane fabricated with NdFeB powder. The volume fraction of powder is 40 %. The right photograph shows a PDMS membrane with embedded magnet.

working principle of these externally actuated electromagnetic micropumps. For the fabrication of the external electromagnet, we used a commercially available coil into which we integrated a soft iron core. The sinusoidal current injected in the electromagnet was used for the actuation of the oscillating membrane containing a rare-earth permanent magnet.

3. MICROFABRICATION METHOD

3.1. Magnetic membrane

For the fabrication of the magnetic membrane, we investigated two possible ways to integrate a NdFeB permanent magnet: (i) a NdFeB/PDMS composite polymer magnet was used for the PMMA micropump (Fig. 2, left and center), while (ii) we integrated a sintered NdFeB magnet for the glass micropump (Fig. 2, right).
In Fig. 3, the measured density curve of the composite magnet is given as a function of the powder volume

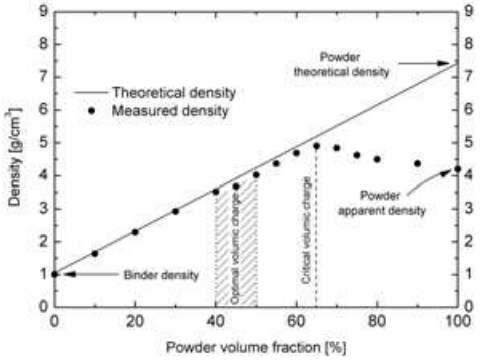

Fig. 3. Relation between the powder volume fraction and the density of the magnet. In terms of homogeneity of the polymer magnet, the optimum volume fraction is obtained for

fraction. These results were obtained for the MQP-S-11-9 spherical NdFeB powder available from Magnequench GmbH. From these experimental data, we could see that a maximum critical charge of about 60 – 70 % could be achieved with such powder. In practice, however, these high-density samples show a non-homogeneous filling. We obtained the best results, in terms of homogeneity, for our fabricated composite magnets with a 40 – 50 % vol. fraction of powder (dashed area in Fig. 3).

3.2. Ball valve micropump in PMMA

We recently demonstrated that the combination of the powder blasting micro-erosion process with standard precision milling tools can be used for the rapid prototyping of multilayered microfluidic chips in PMMA [11,12].
Briefly, the microfabrication process can be described as follows:

- the layers containing the microchannels are structured by powder blasting of thin PMMA sheets protected with a metallic mask;
- the complex parts (ball valve seat and membrane clamp) are fabricated with milling tools;
- the PMMA layers are stacked and bonded together in a hot press by polymerization of a solution of triethylene glycol dimethacrylate (Fluka Chemie AG, Buchs, Switzerland) heated at 70 °C.

During this last step, the PDMS membrane is mechanically clamped in between the central PMMA plates, which ensures a tight sealing of the pumping chamber. A photograph of the assembled ball valve micropump in PMMA is shown in Fig. 4. Note that the prototype consists of a stack of 7 PMMA layers.

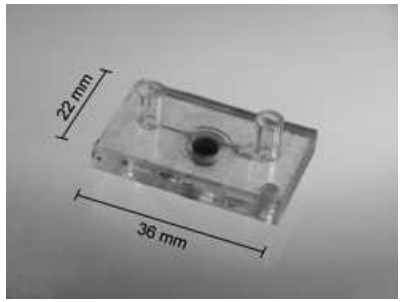

Fig. 4. Photograph of the ball valve micropump made out of PMMA (external dimensions: 36 mm × 22 mm).

3.3. Ball valve micropump in glass

For the fabrication of the glass prototype, we have taken advantage of the udder-like shape obtained by

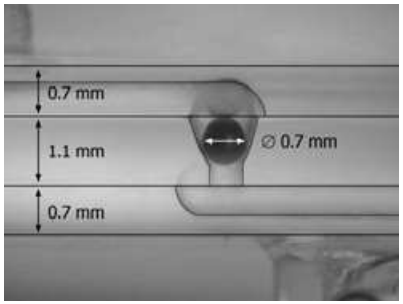

Fig. 5. Photograph of the ball valve integrated in the glass microfluidic chip (Ø 0.7 mm stainless steel ball).

"natural" shape of the holes is found to be particularly suitable for ball valve seats, as illustrated in Fig. 5. All the details on the fabrication method of the ball valve micropump in glass can be found in ref. [13].
The main steps in the fabrication process of glass microfluidic chips are:

- microstructuring of the mask protected borosilicate glass layers by powder blasting;
- cleaning of the glass substrates with isopropanol and a piranha solution;
- fusion bonding of the multilayered glass device at 600 °C;
- plasma bonding of the PDMS membrane on the external glass plate;
- gluing of the connectors with an epoxy solution Epo-Tek 301-2 (Epoxy Technology Inc., Billerica, Massachusetts, USA).

4. RESULTS AND DISCUSSION

4.1. Electromagnetic actuation

For the electromagnetic actuation of the membrane, we used a 4800 turns commercial coil having an internal resistance of 370 Ω (Atam Windings s.r.l., Agrate Brianza, Italy). By applying a continuous current in the coil, we could measure the electromagnetic force exerted on (i) the membrane containing the polymer bonded magnet and (ii) the membrane with an embedded sintered magnet. In Fig. 6, we report the results obtained for zero current, for a 50 mA continuous current, and for a 100 mA continuous current. Typically, in the latter case, an electromagnetic force of about 0.5 N was obtained for both types of magnetic membranes. This force can be related to the pressure exerted in the pumping chamber which has a diameter of Ø 7 mm.

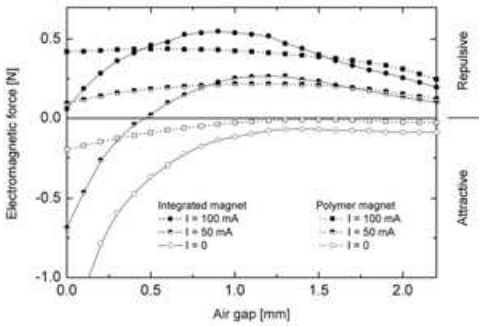

Fig. 6. Dependence of the force generated by the electromagnet as a function of the position of the permanent magnet with respect to the soft magnetic core of the electromagnet (see Fig. 1). The measurements were done for 0 mA (no current), 50 mA and 100 mA continuous current.

4.2. Pumping characteristics

The most interesting characteristics of the diaphragm micropumps are the flow rate – frequency dependence and the back-pressure – frequency dependence curves. In Fig. 7, we report the maximum back-pressure of the two types of ball valve micropumps as a function of the actuation frequency in the case of a 100 mA sinusoidal excitation of the electromagnet. We see that the two prototypes have a resonant frequency in the range of 20 – 30 Hz.
In Fig. 8, we compare the water flow rate of the two prototypes for the same 100 mA sinusoidal excitation of the electromagnet. In this graph, we have included curves that have been calculated from the second order model of the hydrodynamic system described in next section.

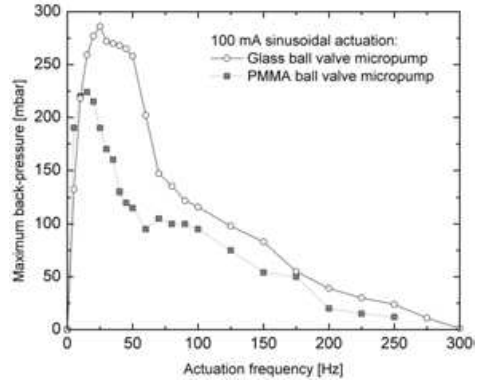

Fig. 7. Comparison of the back-pressure – frequency characteristics of the two types of micropumps. The pumps were actuated with an external electromagnet excited with a

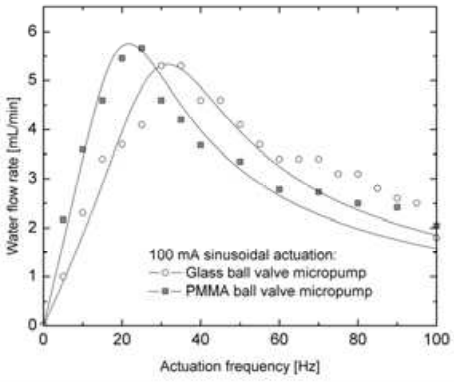

Fig. 8. Comparison of the water flow rate – frequency characteristics of the two types of micropumps. The pumps were actuated with an external electromagnet excited with a 100 mA sinusoidal current. The full lines are calculated using the second order model of section 4.3.

4.3. Damped oscillator model

To estimate the dynamic response of a reciprocating micropump consisting of two passive valves, we can describe the hydraulic system in terms of a simple low-order model. For simplification, the passive valves are considered as ideal fluidic diodes. If we consider, for example, a diaphragm pump working in the fluid ejection phase of the pumping cycle, it can be represented with the schematic diagram of Fig. 9. In this mode, the inlet valve is closed while the outlet valve is opened. If the outlet microchannel has a small section a, high fluid acceleration may be involved and, although the mass of the fluid m is small compared to the mass of the membrane M, its inertial effect is high. If the actuator applies a constant pressure P_S on the flexible membrane of spring constant K, one can predict the acceleration of the fluid in the outlet microchannel. Without leakage or friction losses, and assuming a pressure P_2 in the chamber, we find:

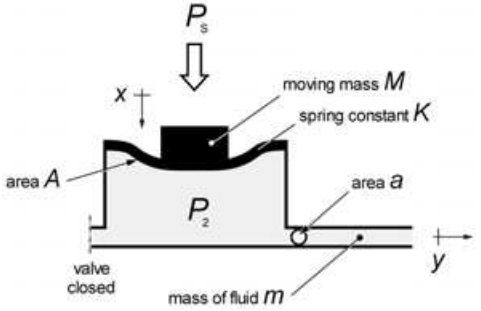

Fig. 9. Schematic diagram of the reciprocating pump showing

$$\left(P_S - P_2\right)A - Kx = M\ddot{x} \tag{1}$$

Neglecting fluid friction, an approximate value for P_2 can be obtained by assuming the fluid in the channel to move as a solid. For a channel of area a containing a total mass m of fluid accelerated at rate $\ddot{y}$, we have:

$$P_2 a = m\ddot{y} \tag{2}$$

Neglecting friction, leakage and compressibility effects, the volume of fluid displaced by the membrane is equal to the volume that flows in the outlet channel, so that:

$$\ddot{y} = \frac{A}{a}\ddot{x} \tag{3}$$

The term $P_2 A$ which appears in eq. (1) can be substituted using the expressions found in eq. (2) and (3). After few manipulations, we easily find that:

$$P_S A = \left\{ M + \left(\frac{A}{a}\right)^2 m \right\} \ddot{x} + Kx \tag{4}$$

From this second order equation, we determine the resonant frequency f_0 of the hydraulic system:

$$f_0 = \frac{1}{2\pi}\sqrt{\frac{K}{M + \left(\frac{A}{a}\right)^2 m}} \tag{5}$$

Note that the factor $(A/a)^2$ may be very high, so that the mass of the membrane could become negligible.

Another method which can be used to model the hydrodynamic system consists in replacing the fluidic elements with their equivalent electrical model [14]. With such approach, the flexible membrane plays the role of a capacitance C with:

$$C = \frac{\Delta V}{P_S - P_2} \tag{6}$$

where the volume variation can be estimated as:

$$\Delta V = Ax \tag{7}$$

Neglecting the inertial effect of the mass M in eq. (1), the membrane deflection is related to the applied pressure by the relation:

$$\left(P_S - P_2\right)A = Kx \tag{8}$$

From eq. (7) and (8), we deduce the capacitance C:

$$C = \frac{A^2}{K} \tag{9}$$

The inertia of the fluid (density ρ) in the outlet microchannel (section a, length l) can be expressed in terms of an inductance L:

$$L = \frac{\rho l}{a} \tag{10}$$

Rewriting the density as $\rho = m/la$, we obtain for the inductance L:

$$L = \frac{m}{a^2} \tag{11}$$

From eq. (9) and (11), we can now calculate the resonant frequency of the system:

$$f_0 = \frac{1}{2\pi}\sqrt{\frac{1}{LC}} = \frac{1}{2\pi}\sqrt{\frac{K}{\left(\frac{A}{a}\right)^2 m}} \tag{12}$$

Here, we have not considered the effect of the mass of the membrane M. Otherwise we would have obtained exactly the same result as in the previous development (eq. (5)).

Finally, to complete the description of the hydraulic system, one can estimate the friction losses in the microchannel from the Hagen-Poiseuille law for laminar flow of incompressible fluids. According to this law, the fluidic resistance R of a pipe of hydraulic diameter D_H and length l is:

$$R = \frac{128\,\mu l}{\pi D_H^4} \tag{13}$$

where μ is the dynamic viscosity of the fluid.

From the RLC electrical equivalent model, the capacitive effect (C) of the pumping chamber, the fluid inertia (L) and the friction losses (R) in the microchannel were calculated for the two prototypes. These data were used in the curves plotted in Fig. 8 and are in excellent agreement with the experiments.

5. CONCLUSION AND OUTLOOK

We have developed and characterized two types of ball valve micropumps realized with the powder blasting microfabrication method. We have also presented an analysis that enables the evaluation of the resonant frequency of diaphragm pumps. The major advantages of ball valves are their reduced leakage ratio, together with the high pressure that these elements are able to withstand. For further improvement of the performance of the ball valve micropump, we suggest the use of spring loaded ball valves, in order to enhance the dynamics of the valves.

References

[1] N.T. Nguyen, X.Y. Huang, and T.K. Chuan, "MEMS-Micropumps: A Review," *ASME J. Fluids Eng.*, **124**, 384-92 (2002).

[2] D.J. Laser and J.G. Santiago, "A Review of Micropumps," *J. Micromech. Microeng.*, **14**, R35-R64 (2004).

[3] M.C. Carrozza, N. Croce, B. Magnani, and P. Dario, "A Piezoelectric-Driven Stereolithography-Fabricated Micropump," *J. Micromech. Microeng.*, **5**, 177-9 (1995).

[4] A. Feustel, O. Krusemark, and J. Müller, "Piezoelectric Membrane Pump with Integrated Ball Valve," *Proc. Actuator '98*, pp. 39-42, Bremen, Germany, June 17-19, 1998.

[5] A. Sin, C.F. Reardon, and M.L. Shuler, "A Self-Priming Microfluidic Diaphragm Pump Capable of Recirculation Fabricated by Combining Soft Lithography and Traditional Machining," *Biotech. Bioeng.*, **85**, 359-63 (2004).

[6] T. Pan, S.J. McDonald, E.M. Kai, and B. Ziaie, "A Magnetically Driven PDMS Micropump with Ball Check-Valves," *J. Micromech. Microeng.* (in press).

[7] X. Dai, M. Pavio, and R.A. Miesem, "Micropump Including Ball Check Valve Utilizing Ceramic Technology and Method of Fabrication," *U.S. patent 6620273*, 2003.

[8] S. Shoji and M. Esashi, "Microflow Devices and Systems," *J. Micromech. Microeng.*, **4**, 157-71 (1994).

[9] O. Krusemark, A. Feustel, and J. Müller, "Micro Ball Valve for Fluidic Micropumps and Gases," *Proc. microTAS '98*, pp. 399-402, Banff, Canada, Oct. 13-16, 1998.

[10] C. Fu, Z. Rummler, and W. Schomburg, "Magnetically Driven Micro Ball Valves Fabricated by Multilayer Adhesive Film Bonding," *J. Micromech. Microeng.*, **13**, S96-S102 (2003).

[11] C. Yamahata, M. Chastellain, V.K. Parashar, A. Petri, H. Hofmann, and M.A.M. Gijs, "Plastic Micropump with Ferrofluidic Actuation," *J. Microelectromech. Syst.*, **14**, 96-102 (2005).

[12] C. Yamahata, C. Lotto, E. Al-Assaf, and M.A.M. Gijs, "A PMMA Valveless Micropump Using Electromagnetic Actuation," *Microfluidics and Nanofluidics* (in press). DOI: 10.1007/s10404-004-0007-6

[13] C. Yamahata, F. Lacharme, Y. Burri, and M.A.M. Gijs, "A Ball Valve Micropump in Glass Fabricated by Powder Blasting," *Sens. Actuators B* (in press). DOI: 10.1016/j.snb.2005.01.005

[14] T. Bourouina and J.-P. Grandchamp, "Modeling Micropumps with Electrical Equivalent Networks," *J. Micromech. Microeng.*, **6**, 398-404 (1996).